

Repeat bathymetric surveys at 1-metre resolution of lava flows erupted at Axial Seamount in April 2011

David W. Caress^{1*}, David A. Clague¹, Jennifer B. Paduan¹, Julie F. Martin¹, Brian M. Dreyer², William W. Chadwick Jr³, Alden Denny⁴ and Deborah S. Kelley⁴

At sites with frequent submarine volcanic activity, it is difficult to discern between new and pre-existing lava flows. In particular, the distribution of the fissures from which lava erupts, the routes taken by lava flows and the relationship between the new flows and the pre-existing seafloor bathymetry are often unclear. The volcanic and hydrothermal systems of Axial Seamount submarine volcano in the Pacific Ocean have been studied intensively since eruptions were detected in 1998 (refs 1,2) and 2011 (ref. 3). Here we combine pre- and post-eruption bathymetric surveys^{3–8}, with 1-m lateral resolution and 0.2-m vertical precision, to precisely map the extent and thickness of the lava flows, calculate the volume of lava and unambiguously identify eruptive fissures from the April 2011 eruption. Where the new lava flows extend beyond the boundaries of the repeated surveys, we use shipboard multibeam surveys to map the flows with lower resolution. We show that the eruption produced both sheet and lobate flows associated with high eruption rates and low-eruption-rate pillow mounds. We find that lava flows erupted from new as well as existing fissures and tended to reoccupy existing flow channels. This reoccupation makes it difficult to map submarine flows produced during one eruption without before-and-after bathymetric surveys.

Axial Seamount is a large volcanic edifice situated at the junction of the Cobb hotspot trace with the Juan de Fuca Ridge spreading centre. The summit (Fig. 1) is characterized by a prominent 3- by 8-km horseshoe-shaped caldera that is more than 100 m deep at its north end and overflowed by recent eruptions along its southern margin⁹. Observations of the 1998 eruption^{2,10–13} with attendant seismic and geodetic signals, large lava flows and subsequent changes in hydrothermal activity led to sustained observatory and expeditionary studies of the geology and hydrology of the seamount^{1,14,15}. One aspect of these studies was the collection of near-bottom 1-m-resolution bathymetric mapping of the summit, including the caldera floor and rim, and the upper south rift zone, during 13 surveys in 2006–2009 using the autonomous underwater vehicle (AUV) *D. Allan B.* (ref. 8; Fig. 1).

A second historical eruption on Axial Seamount began on 6 April 2011 and lasted for six days, but was not discovered until late July during a remotely operated vehicle (ROV) *Jason* dive in the southern caldera. This discovery, and the data from *in situ* bottom-pressure recorders and ocean-bottom hydrophones that revealed the timing of the eruption, are presented in recent studies^{3,16}. Within a week after recognition of the eruption, the AUV *D. Allan B.*

mapped the flows in and near the caldera in surveys designed using the observations of new lava and missing instruments^{3,16}. The 2011 post-eruption survey mostly overlies the pre-eruption coverage collected in 2006–2009, allowing unequivocal identification of the extent and thickness of the new lava flows as a depth-difference map (Fig. 2a–c), and the flow morphology. The difference map can resolve flow thicknesses as thin as 0.2 m. From these data we interpreted the flow margins and eruptive fissure locations (Fig. 2d). The high-resolution maps in turn guided ROVs *Doc Ricketts* and *ROPOS* dives to confirm the distribution of new lava with video observations and samples. During the *ROPOS* dive programme in August, shipboard 30-kHz multibeam data collected by the research vessel (RV) *Thompson* on Axial allowed lower-resolution detection, outside the AUV coverage, of seafloor changes owing to emplacement of new lava when compared with a survey in May 1998 (ref. 17).

Similar techniques have been applied previously using lower-resolution bathymetry data collected during repeat surveys from ships^{18–20}. Pre- and post-eruption sidescan and bottom photography of the 2005–2006 eruption at 9° 50' N on the East Pacific Rise were used to map the extent and estimate the thickness and volume of the new flows^{21,22}, but near-bottom 5-m lateral, 1-m vertical resolution bathymetry were collected only before that eruption²³ and only for <2 km². One-metre-resolution bathymetric surveys have been completed for only a few small sections of the global ridge system, and Axial Seamount is the only location where both pre- and post eruption surveys have been collected.

The 2011 flows erupted from multiple, discontinuous *en echelon* fissures (Fig. 2d), most aligned perfectly with at least six different fissures present before the 2011 eruption. Some of the fissures increased in width as much as 7 m (to become 16 m wide in one place) and increased in depth as much as 10 m (to become 18 m deep in one place). Fissure eruptions at Kilauea and Mauna Loa volcanoes create new, often closely parallel, fissures, but reoccupation, deepening and widening of the same fissures has not been documented, nor has the remarkable and exact reoccupation of multiple fissures from different eruptions. The fissures extend 10 km from their north end on the eastern caldera rim to the south near the 1998 south rift lava flow²⁴. A 1,050-m-long new ridge (labelled A on Fig. 2d) at the south end of the *en echelon* fissure system (mapped only in part by the new 1-m-resolution surveys) is located astride a wide fissure seen in the pre-eruption bathymetry, but is located north of the section of this same fissure that erupted in 1998. Newly formed fissures erupted only

¹Monterey Bay Aquarium Research Institute, 7700 Sandholdt Road, Moss Landing, California 95039, USA, ²University of California Santa Cruz, Institute of Marine Sciences, 1156 High St., Santa Cruz, California 95064, USA, ³Oregon State University/CIMRS, 2115 SE OSU Drive, Newport, Oregon 97365, USA,

⁴University of Washington, School of Oceanography, Seattle, Washington 98195, USA. *e-mail: caress@mbari.org.

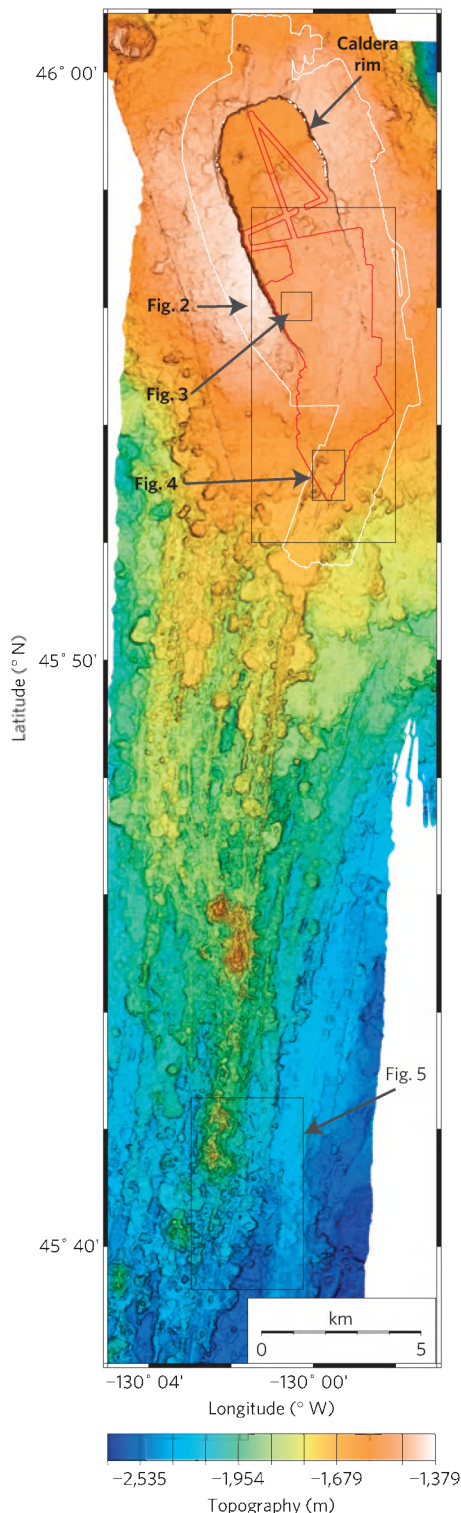


Figure 1 | Post-eruption Axial Seamount bathymetry combining high-resolution bathymetry collected by AUV and EM302 data gridded at 5-m spacing. The extent of the pre- and post-eruption high-resolution surveys is shown using white and red outlines, respectively. Boxes show the extents of Figs 2–5.

at the northern end of the fissure system on the east rim of the caldera and just north of ridge A. Fissure segments have lengths from 60 to 570 m. Lateral offsets in the fissures (Fig. 2d) jump eastwards and then westwards, and are as large as 300 m, resulting in discontinuous surface flows. The southernmost fissures are

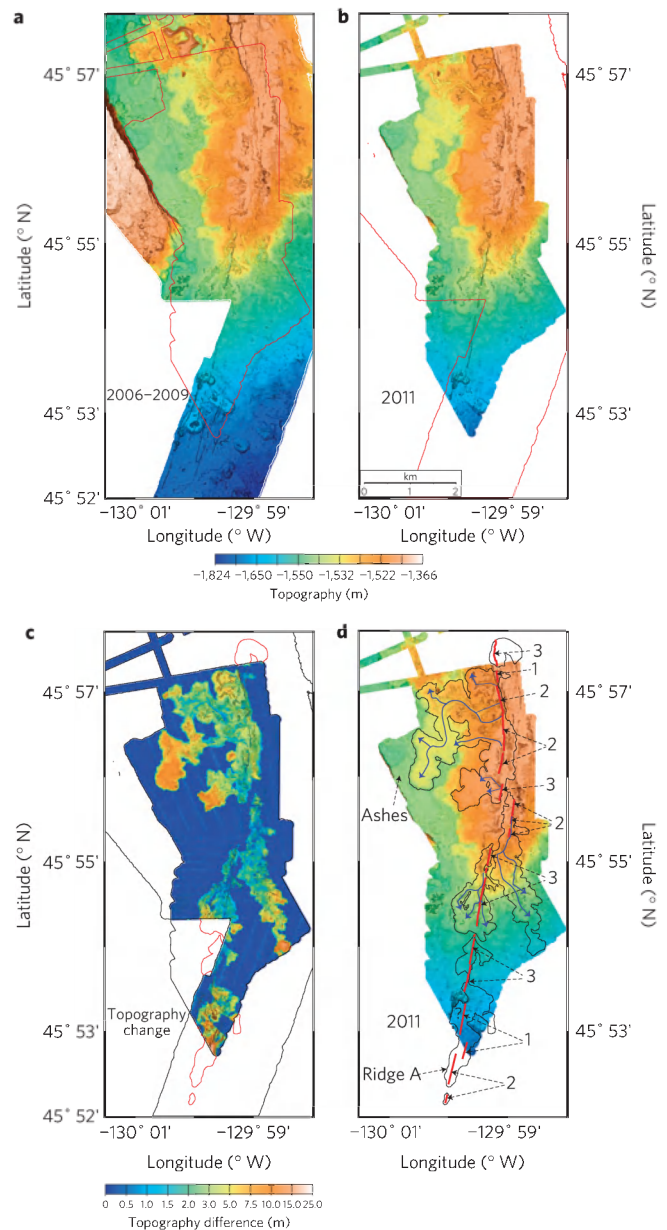


Figure 2 | High-resolution bathymetry of the summit flows gridded at 1-m resolution. **a**, Map showing pre-eruption bathymetry with the area mapped in 2011 outlined by a red line. **b**, Map showing post-eruption bathymetry with the area mapped in 2006–2009 outlined by a red line. **c**, The lava flows are defined using the difference between pre- and post-eruption bathymetry. Red lines show flow margins outside the high-resolution coverage inferred from hull-mounted multibeam and backscatter data. **d**, The post-eruption bathymetry from **b** with an interpretive overlay showing the flow margins as black outlines. Eruptive fissures shown in red with 1, new fissures; 2, reoccupied 1998 fissures²⁶; and 3, reoccupied pre-1998 fissures. Lava flow channels are shown in blue. The longest channel (3.6 km) terminated adjacent to Ashes hydrothermal vent field. Pillow ridge A referred to in the text is labelled. The exact location of the fissure labelled '?' is uncertain because it is buried by lava. All maps are scaled the same. The topography colour bar applies to **a**, **b**, **d**. The topography difference colour bar applies to **c**.

oriented 15° (measured clockwise relative to north), identical to the underlying 1998 fissure, but rotate anticlockwise at the northern end to 346°–353°, similar to the roughly 342° orientation of the nearby caldera rim.

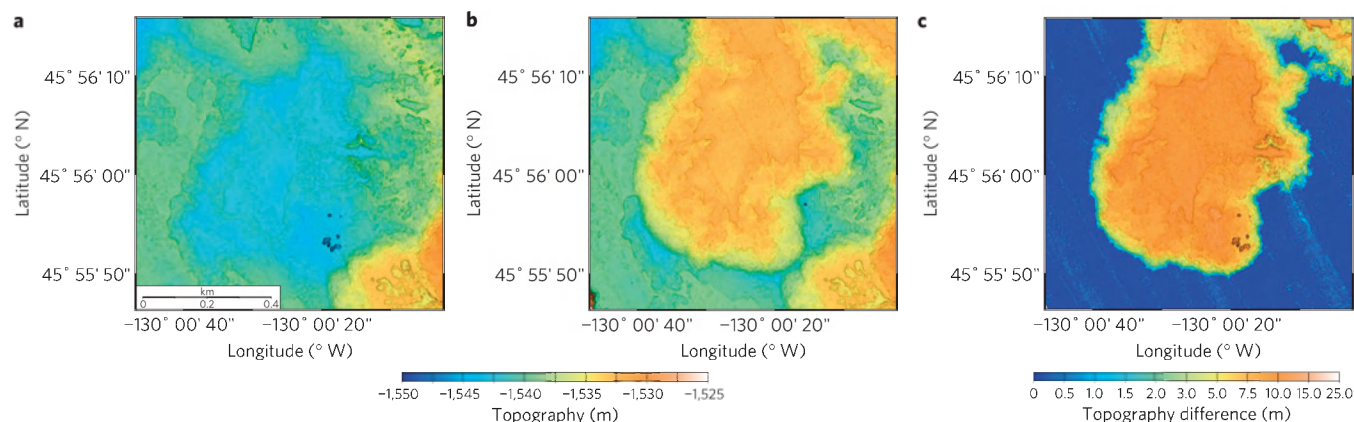


Figure 3 | High-resolution bathymetry for a small area located at the southwest corner of the caldera (see Fig. 1 for location). a, Pre-eruption bathymetry from 2006–2009 surveys. **b,** Post-eruption bathymetry from 2011 surveys. **c,** Bathymetric difference map showing the extent and thickness of the 2011 lava in this region. Here the flow filled a shallow depression and inflated, attaining a 15-m thickness. All maps are scaled the same.

At the north end of the eruption area, sheet and lobate flows from a new fissure on the caldera rim cascaded westwards into the caldera forming a small mound of lava at the base of the caldera wall and were observed draping the 20–25-m-high caldera wall. This same flow extends east away from the caldera, but was incompletely mapped by the *D. Allan B.* Here, the flows are generally <5-m thick from comparison of the pre-eruption AUV survey and bathymetry collected from the RV *Thompson* after the eruption. As with most sheet flows at Axial, channels of jumbled lava morphology are surrounded by higher-standing, uncollapsed lobate margins.

The three large summit lava flows observed during ROV dives were emplaced as lobate sheet flows that initially ponded 4–5 m deep near their eruptive fissures, and then drained and collapsed as the flows advanced down channels, mainly to the west. Positive depth differences everywhere within pre-existing drained areas show that the 2011 lava completely flooded these pre-existing channel systems and then quickly drained away, leaving vertical pond walls and lava pillars as tall as 5 m. Other channels in the new flows followed and smoothed previous channels with levees or channels of drained, jumbled sheet flows, similar to descriptions of reoccupation of channels in the 2005–2006 9° 50' N flows^{21,22}. Most channels and flows mimic the morphology of previous lava flows to a remarkable degree, including the 1998 sheet flow²⁴. Beyond the near-vent sheet flows with collapses and channels, the overflows and distal portions transition to inflated lobate flows that thicken dramatically towards their distal ends, reaching thicknesses of 10–15 m compared with near-vent sheet flows that are only <1 m to several metres thick. A distal inflated lobe emplaced adjacent to the Ashes hydrothermal field is prominent in the difference map (Figs 2 and 3). This flow was fed through a 3.6-km-long zigzag channel and the upper portions follow channels in the underlying 1998 lava flow (Fig. 2d). Near the southernmost portion of the 2011 lava flows on the upper south rift zone, the flows fill some existing fissures and collapse areas to 15–16 m deep (Fig. 4).

Other than the sheet flows in the channels, most of the 2011 lavas in the caldera and upper south rift have lobate morphology and cover pre-existing sheet flows, partially filling existing channels. ROV observations indicate that the lobate flows typically have about 25–50 m margins of small pillow lavas, as described previously at the East Pacific Rise^{21–23}. The summit flows cover an area $7.8 \times 10^6 \text{ m}^2$ and contain a volume of $27 \times 10^6 \text{ m}^3$ of freshly erupted lava. The average flow thickness is 3.5 m, the maximum thickness is 17 m and 11% of the new flows by area are <1 m thick.

A 2-km long, 30-m thick ridge (labelled A on Fig. 2d) on the south rift zone extends beyond the AUV survey but is covered by shipboard multibeam. ROV exploration confirmed it is made of

new pillow lavas. This ridge has an area of $0.6 \times 10^6 \text{ m}^2$ and consists of $6.2 \times 10^6 \text{ m}^3$ of new lava, with an average thickness of 10 m and a maximum thickness of 26 m. The comparison of 1998 and 2011 shipboard multibeam also reveals a second ridge (labelled B in Fig. 5) that is 4.8 km long and up to 137 m thick and whose northern end is 18.5 km south of the southern end of ridge A. Hydroacoustic data showed that the dyking event associated with the 1998 eruption extended 50 km down the south rift beyond ridge B (ref. 10). Seismic data from the US Navy Sound Surveillance System (SOSUS) hydrophone array data available from 1998 to December 2009 and ocean-bottom hydrophones since then¹⁶, as well as seafloor deformation observations in the caldera from 2000 to the April 2011 eruption^{3,15}, detected signals associated with intrusion or eruption only during the two known eruptions in 1998 and 2011; therefore we conclude that ridge B is most probably part of the 2011 eruption. RV *Thompson* dredged ridge B in October 2011 and the samples are being dated using the ^{210}Po – ^{210}Pb technique to establish when this feature erupted (K. Rubin, personal communication). Ridge B averages 38 m thick, covers $1.7 \times 10^6 \text{ m}^2$ and contains $66 \times 10^6 \text{ m}^3$ of plagioclase-phyric fresh basalt, making it distinct from the aphyric basalt sampled from the other 2011 flows, and twice the volume erupted near the summit.

If ridge B is included, the 2011 Axial Seamount flows cover an area of 10.1 km^2 and have a volume of 0.099 km^3 . The 2011 flows erupted from an *en echelon* fissure system that extended semicontinuously for 10 km from the eastern rim of the summit caldera (33.3 km discontinuously including ridge B). In comparison, the 1998 lavas erupted from two separate fissure systems, one 3.8-km long and the other 1.4-km long, extending 9.9 km in total length²⁴.

The 2011 flows are dominantly lobate and sheet flows near the summit similar to those erupted during the much less voluminous 1998 eruption²⁴. Their thinness and flow morphology near the eruptive vents and within channels, long flow lengths (up to 3.6 km from the vents, Fig. 2d) and thick distal ends all suggest they were emplaced rapidly. In contrast, the pillow ridges, especially the one on the lower south rift where two-thirds of the volume of new lava was erupted, were probably emplaced more slowly and over a longer period of time. Thus, the 2011 eruption consisted of both high-eruption-rate sheet and lobate flows and low-eruption-rate pillow mounds, in contrast to all other documented eruptions that consist of one or the other^{21,22,25}. The early high-effusion-rate part of the eruption may have depleted magma stored at shallow depths of volatiles such as CO_2 , leading to later, lower-effusion-rate production of pillow lava²⁶.

The extent to which pre-existing, drained, near-fissure, ponded flows and channels were reoccupied is similar to observations

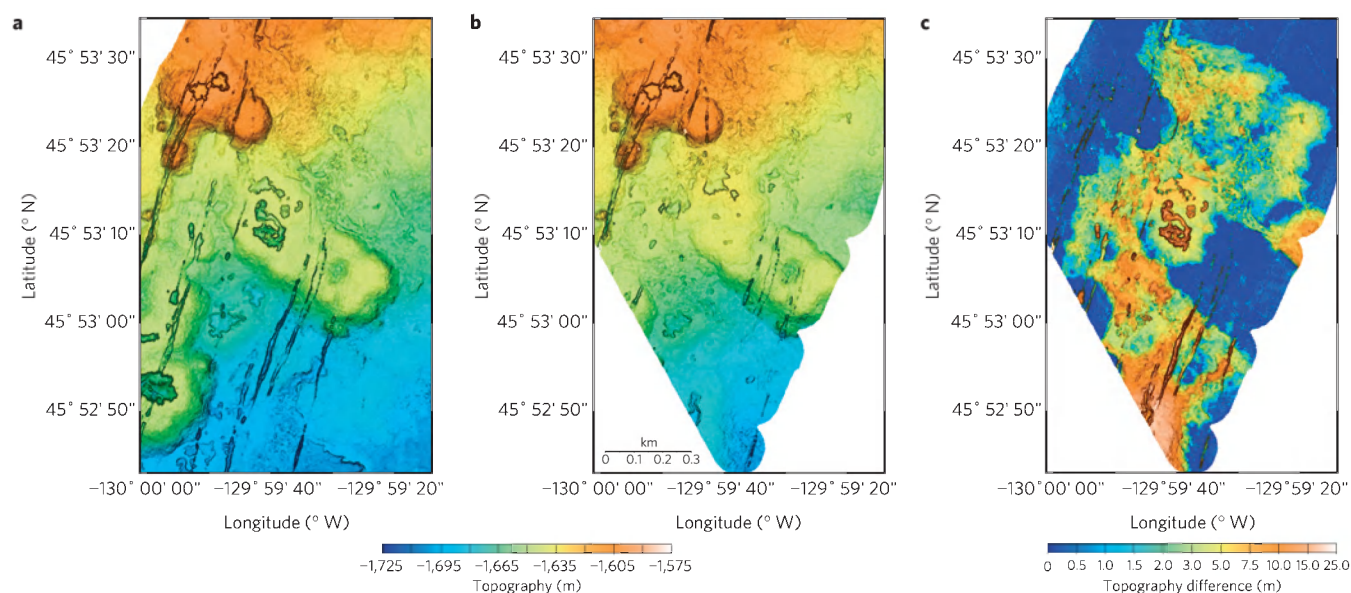


Figure 4 | High-resolution bathymetry for a small area south of the caldera on the upper south rift zone (see Fig. 1 for location). a. Pre-eruption bathymetry from 2006–2009 surveys. **b.** Post-eruption bathymetry from 2011 surveys. **c.** Bathymetric difference map showing the extent and thickness of the 2011 lava in this region. The flow erupted from pre-existing fissures and filled several old fissures, tectonic fractures and collapse features in the centre of a low pillow mound. The flow thickened into a pillow ridge (referred to as ridge A in the text) to the south, which partly lies outside the high-resolution repeat mapping coverage. All maps are scaled the same.

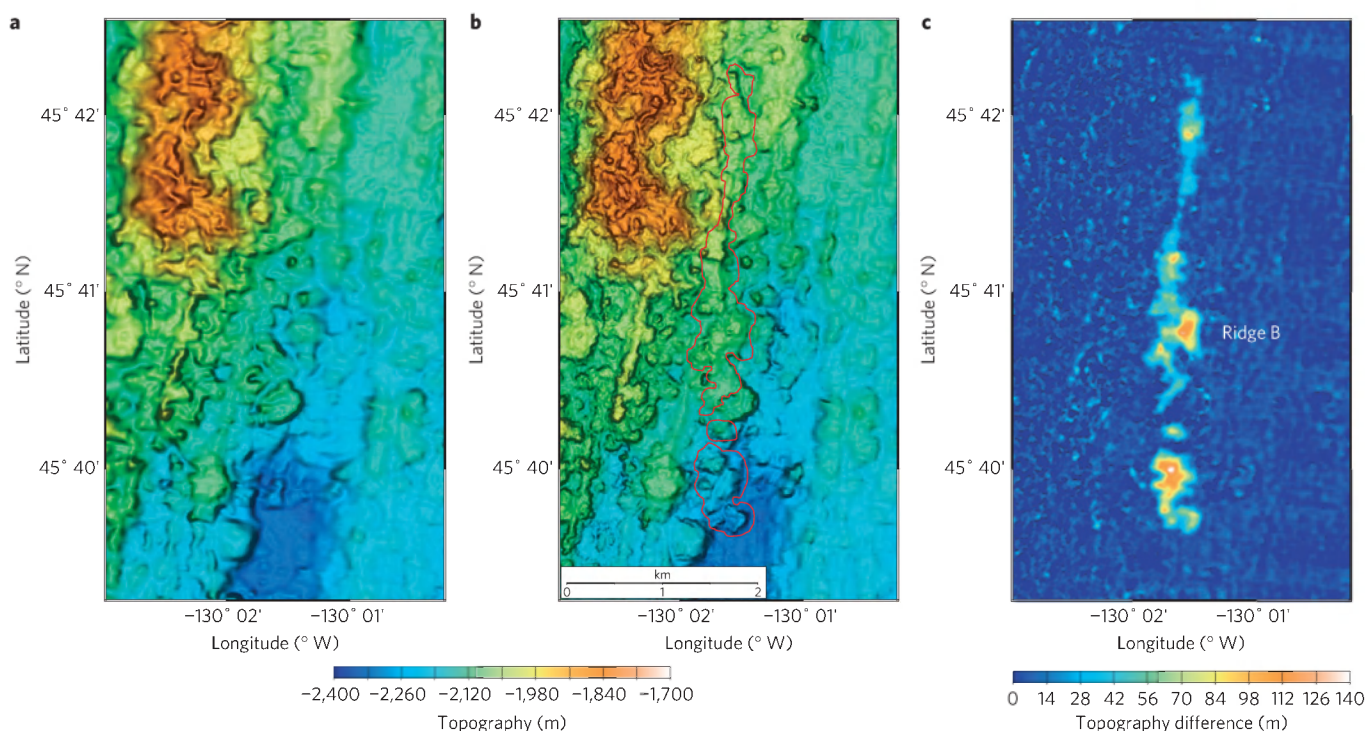


Figure 5 | Shipboard multibeam bathymetry of the southern ridge, referred to as ridge B in the text, gridded at 5-m spacing. a. Pre-eruption 70-m-resolution bathymetry from EM300 multibeam data¹⁷. **b.** Post-eruption 35-m-resolution bathymetry from EM302 multibeam data. The flow margin is shown in red. **c.** Bathymetric difference map. Ridge B is as much as 137 m thick and is interpreted to have formed as part of the April 2011 eruption. All maps are scaled the same.

along the East Pacific Rise^{21–23}, but eruptive fissures from previous eruptions were also reoccupied. The Axial flows covered the area completely, leaving only rare kipukas, in contrast to the dozens observed in the 2005–2006 flows on the East Pacific Rise²². Likewise, evidence for drainback into the eruptive fissures is restricted to deep fissures on the uppermost rift zone south of the caldera in the

2011 flows, compared with widespread observations of drainback at fissures on the East Pacific Rise^{21–23,27}. The reoccupation of the drained ponds and channels at Axial is a consequence of the same fissures being reactivated. This characteristic, where subsequent flows mimic earlier ones, complicates our ability to map submarine flows produced during single eruptions where we lack

before-and-after bathymetry. For example, it would now be much more difficult to map the 1998 summit flows²⁴ as distinct from the 2011 flows. The composite character of at least some mapped flows may explain the difference between a recurrence interval of 13 years based on the 1998 and 2011 eruptions, and ~33 years based on mapping of 11 flows younger than ~360 years within the caldera⁷.

Methods

The *D. Allan B.* is a torpedo-shaped, 5.2-m-long, 6,000-m-depth-rated AUV designed and constructed by the Monterey Bay Aquarium Research Institute for high-resolution seafloor surveys⁸. The vehicle carries a 200-kHz 1° × 1° beam-width multibeam sonar, 110-kHz chirp sidescan sonar, 1–6-kHz chirp sub-bottom profiler, magnetometer and conductivity, temperature and depth (CTD) sensor for 17.5-h missions at 1.5 m s⁻¹ speed. The near-bottom surveys were run at an altitude of 50 m, yielding bathymetry with 1-m lateral resolution. Real-time navigation was provided by an inertial navigation system aided by velocity-over-bottom data from a Doppler velocity log sonar and depth data from a pressure sensor; the inertial navigation was accurate relative to the starting location to 0.05% of distance travelled, or better than 35 m during the ~70-km-long surveys. However, the initial AUV location was set by acoustic modem communication using tracking from an ultra-short-baseline sonar and thus the absolute accuracy of the initial navigation was limited by the ultra-short-baseline fix precision of roughly 50–100 m.

The mapping data were processed using the MB-System software package^{8,17,28,29}. All multibeam data were corrected for tides using pressure data from a bottom-pressure recorder deployed inside the caldera⁷. The program MBnavadjust was used to adjust the AUV navigation by lateral translations of as much as 85 m so that features match in overlapping bathymetry swaths. Most AUV missions required correction for dive-specific static pressure depth offsets less than 0.5 m; two missions had offsets of about 5 m. The pre- and post-eruption surveys were co-registered by matching features away from the new lava flows. The AUV bathymetry were also co-registered with the EM302 bathymetry collected by the *RV Thompson*. The EM302 data are lower resolution but global-positioning-system navigated, so co-registration improved the AUV navigation accuracy in an absolute sense. The final navigation is accurate in a relative sense to 1 m, in an absolute sense to 35 m (the lateral resolution of the EM302 bathymetry) and has a vertical precision of 0.1 m. The difference maps used to identify the new lava flows have a vertical precision of 0.2 m, consistent with noise in regions of no change. Flow volumes were calculated by two methods that yielded similar results. The values reported here were calculated by integrating the bathymetric difference within the manually drawn flow boundaries shown in Fig. 2d. The second method used as a quality check was to integrate the bathymetric difference wherever the difference exceeded the detection threshold of +0.2 m.

Hull-mounted 30-kHz multibeam data used outside the high-resolution coverage collected from the AUV were collected four months after both the 1998 and 2011 eruptions. The 1998 surveys used a 2° × 2° beam width EM300 multibeam (*RV Ocean Alert*)¹⁷ and the 2011 surveys used a 1.0° × 1.0° beam width EM302 multibeam (*RV Thompson*). No intervening surveys of the south rift were conducted. The footprint-weighted mean algorithm of MBgrid was used to incorporate the beam footprint geometry of each sounding in the gridding process. Thus, although grids combining high-resolution and shipboard multibeam data were calculated with a 5-m grid cell size, the features mapped only by shipboard multibeam are resolved to the beam footprint scales of 50 m at the summit to 70 m at the southern end of Fig. 1 for the EM300 and 25–35 m for the EM302.

Bottom observations and samples from ROV dives conducted during summer 2011 confirm the new lava flows inferred from the repeat mapping. These include ROV *Jason* dives J2-580, J2-581 and J2-583, ROV *Doc Ricketts* dives D254 and D270, and ROV *ROPOS* dives R1467, R1469, R1470, R1472 and R1473. Dredge D01 from ridge B was recovered by *RV Thompson* during transit TN271.

Received 25 January 2012; accepted 11 May 2012; published online 10 June 2012

References

- Chadwick, J. *et al.* Magmatic effects of the Cobb hotspot on the Juan de Fuca Ridge. *J. Geophys. Res.* **110**, B03101 (2005).
- Embley, R. W., Chadwick, W. W. Jr, Clague, D. & Stakes, D. The 1998 Eruption of Axial Volcano: Multibeam anomalies and seafloor observations. *Geophys. Res. Lett.* **26**, 3425–3428 (1999).
- Chadwick, W. W. Jr, Noonan, S., Butterfield, D. A. & Lilley, M. D. Seafloor deformation and forecasts of the April 2011 eruption at Axial Seamount. *Nature Geosci.* <http://dx.doi.org/10.1038/ngeo1464> (2012).
- Thomas, H. *et al.* Mapping AUV survey of Axial Seamount. *Eos Trans. AGU (Fall Meeting Suppl.)* **87**, Abstract V23B-0615 (2006).
- Caress, D. W. *et al.* AUV mapping of Axial Seamount, Juan de Fuca Ridge: The northern caldera floor and northeast rim. *Eos Trans. AGU (Fall Meeting Suppl.)* **88**, Abstract T33B-1355 (2007).
- Clague, D. A. *et al.* AUV mapping of Axial Seamount, Juan de Fuca Ridge: The southern caldera floor and upper south rift. *Eos Trans. AGU (Fall Meeting Suppl.)* **88**, Abstract T33B-1354 (2007).
- Clague, D. A., Paduan, J. B., Dreyer, B. M., Caress, D. W. & Martin, J. High-resolution AUV mapping and lava flow ages at Axial Seamount. Abstract V14C-05 presented at 2011 Fall Meeting, AGU, San Francisco, California, 5–9 Dec. (2011).
- Caress, D. W. *et al.* in *Marine Habitat Mapping Technology for Alaska* (eds Reynolds, J. R. & Greene, H. G.) (Alaska Sea Grant College Program, University of Alaska Fairbanks, 2008); <http://dx.doi.org/10.4027/mhmta.2008.04>.
- Embley, R. W., Murphy, K. M. & Fox, C. G. High-resolution studies of the summit of Axial Volcano. *J. Geophys. Res.* **95**, 12785–12812 (1990).
- Dziak, R. P. & Fox, C. G. The January 1998 earthquake swarm at Axial Volcano, Juan de Fuca Ridge: Hydroacoustic evidence of seafloor volcanic activity. *Geophys. Res. Lett.* **26**, 3429–3432 (1999).
- Fox, C. G. *In situ* ground deformation measurements from the summit of Axial Volcano during the 1998 volcanic episode. *Geophys. Res. Lett.* **26**, 3437–3440 (1999).
- Fox, C. G., Chadwick, W. W. Jr & Embley, R. W. Direct observation of a submarine volcanic eruption from a sea-floor instrument caught in a lava flow. *Nature* **412**, 727–729 (2001).
- Chadwick, W. W. Jr, Embley, R. W., Milburn, H. B., Meinig, C. & Stapp, M. Evidence for deformation associated with the 1998 eruption of Axial Volcano, Juan de Fuca Ridge, from acoustic extensometer measurements. *Geophys. Res. Lett.* **26**, 3441–3444 (1999).
- Chadwick, W. W. Jr, Noonan, S., Zumberge, M., Embley, R. W. & Fox, C. G. Vertical deformation monitoring at Axial Seamount since its 1998 eruption using deep-sea pressure sensors. *J. Volcanol. Geotherm. Res.* **150**, 313–327 (2006).
- Noonan, S. L. & Chadwick, W. W. Jr Volcanic inflation measured in the caldera of Axial Seamount: Implications for magma supply and future eruptions. *Geochem. Geophys. Geosyst.* **10**, Q02002 (2009).
- Dziak, R. P., Haxel, J. H., Bohnenstiehl, D. & Matsumoto, H. Seismic precursors and magma ascent before the April 2011 eruption at Axial Seamount. *Nature Geosci.* <http://dx.doi.org/10.1038/ngeo1490> (2012).
- MBARI Mapping Team *Seamounts and Ridges Multibeam Survey* (Monterey Bay Aquarium Research Institute Digital Data Series No. 7, 1-CD, 2001).
- Chadwick, W. W. Jr, Embley, R. W. & Fox, C. G. Evidence for volcanic eruption on the southern Juan de Fuca Ridge between 1981 and 1987. *Nature* **350**, 416–418 (1991).
- Fox, C. G., Chadwick, W. W. Jr & Embley, R. W. Detection of changes in ridge-crest morphology using repeated multibeam surveys. *J. Geophys. Res.* **97**, 11149–11162 (1992).
- Chadwick, W. W. Jr, Embley, R. W. & Shank, T. M. The 1996 Gorda Ridge eruption: Geologic, mapping, sidescan sonar, and SeaBeam comparison results. *Deep Sea Res. II* **45**, 2547–2566 (1998).
- Soule, S. A., Fornari, D. J., Perfit, M. R. & Rubin, K. H. New insights into mid-ocean ridge volcanic processes from the 2005–2006 eruption of the East Pacific Rise, 9° 46' N–9° 56' N. *Geology* **35**, 1079–1082 (2007).
- Fundis, A. T., Soule, S. A., Fornari, D. J. & Perfit, M. R. Paving the seafloor: Volcanic emplacement processes during the 2005–2006 eruptions at the fast spreading East Pacific Rise, 9° 50' N. *Geochem. Geophys. Geosyst.* **11**, Q08024 (2010).
- Fornari, D. J. *et al.* Submarine lava flow emplacement at the East Pacific Rise 9° 50' N: Implications for uppermost Ocean crust stratigraphy and hydrothermal fluid circulation. *Geophys. Monogr. AGU* **148**, 182–217 (2004) 311.
- Chadwick, W. W. *et al.* High-resolution mapping of the 1998 lava flows at Axial Seamount. Abstract OS11C-01 presented at 2011 Fall Meeting, AGU, San Francisco, California, 5–9 Dec. (2011).
- Chadwick, W. W. Jr, Scheirer, D. S., Embley, R. W. & Johnson, H. P. High-resolution bathymetric surveys using scanning sonars: Lava flow morphology, hydrothermal vents, and geologic structure at recent eruption sites on the Juan de Fuca Ridge. *J. Geophys. Res.* **106**, 16075–16099 (2001).
- Clague, D. A., Paduan, J. B. & Davis, A. S. Widespread strombolian eruptions of mid-ocean ridge basalt. *J. Volcanol. Geotherm. Res.* **180**, 171–188 (2009).
- Sinton, J. *et al.* Volcanic eruptions on mid-ocean ridges: New evidence from the superfast spreading East Pacific Rise, 17°–19° S. *J. Geophys. Res.* **107**, 1–21 (2002).
- Caress, D. W. & Chayes, D. N. Improved processing of Hydrosweep DS Multibeam Data on the R/V Maurice Ewing. *Mar. Geophys. Res.* **18**, 631–650 (1996).
- Caress, D. W. & Chayes, D. N. *MB-System: Mapping the Seafloor* Open source software distributed from the MBARI and L-DEO web sites (2011); <http://www.mbari.org/data/mbsystem/>.

Acknowledgements

A grant from the David and Lucile Packard Foundation to the Monterey Bay Aquarium Research Institute and a contribution from J. Delaney (Univ. Washington) supported

acquisition of the 2011 AUV *D. Allan B.* data. We thank the MBARI AUV operations group consisting of H. Thomas, D. Conlin and D. Thompson for conducting the AUV surveys. We thank the captains and crews of the RVs *Zephyr*, *Western Flyer*, *Thompson* and *Atlantis*, and the pilots of the ROVs *Jason*, *Doc Ricketts* and *ROPOS* for their flexibility and support as plans changed to collect the 2011 AUV surveys and explore and sample the new flows. The pre-eruptive AUV *D. Allan B.* data were collected during cruises on the RV *Thompson* in 2006 and RV *Atlantis* in 2007 and 2008 under chief scientists B. Chadwick, D. Butterfield and J. Holden, respectively. The 2009 AUV *D. Allan B.* data collected from the RV *Zephyr* completed the pre-2011 eruption mapping of the summit and upper south rift zone on Axial Seamount. B.M.D. was supported by NSF award OCE-1061176. PMEL contribution 3791.

Author contributions

D.W.C. designed the AUV surveys, did most of the data processing, constructed the figures and co-wrote the manuscript and revisions; D.A.C. adjusted ship commitments to

collect the 2011 survey data, defined the areas to be covered based on sparse observations of the new flow, designed and ran ROV *Doc Ricketts* dives to observe and collect the new flows and co-wrote the manuscript and revisions; J.B.P. and J.F.M. assisted with data processing at sea and post-cruise, measured features and calculated areas and volumes of the flows and edited the manuscript; B.M.D. interpreted the pre-eruptive AUV data to define flow units and assisted at sea in 2011; W.W.C. provided the key information to D.A.C. while both were at sea in 2011 that enabled the AUV surveys to take place, calculated flow areas and volumes and contributed to writing the manuscript; A.D. and D.S.K. collected the post-eruption EM302 multibeam data and key ROV *ROPOS* observations and samples of the new flows.

Additional information

The authors declare no competing financial interests. Reprints and permissions information is available online at www.nature.com/reprints. Correspondence and requests for materials should be addressed to D.W.C.